Nano Ferrites Microwave Complex Permeability and Permittivity Measurements by T/R Technique in Waveguide

Mahmut Obol, Nawaf Al-Moayed, Usman A. Khan, Mohammed N. Afsar

High Frequency Materials Measurement and Information Center, and Department of Electrical Engineering, Tufts University, Medford, MA 02155

Mahmut.Obol@tufts.edu

***Abstract* — There is a huge demand to accurately determine the magneto-electrical properties of particles in the nano sized regime due to the modern IC technology revolution and biomedical application science. In this paper, we present a microwave waveguide measurement technique for complex permeability and permittivity of expensive nano sized magnetic powder materials. In the measurement process, Agilent's 8510C vector network analyzer was used to have a standard TRL calibration for free space inside the waveguides. In order to maintain the recommended insertion phase range, a very thin prepared sample was loaded inside the calibrated waveguide. Also, the loaded material's magnetic and dielectric effects were considered into the cutoff wavelength of the propagation constant of the TE_{10} wave from the geometrical dimensions of the waveguides. This makes the measured permeability and permittivity more reliable than commonly used techniques. The six different compounds of nano sized ferrite powders (Fe_3O_4, $CuFe_2O_4$, $CuFe_2O_4Zn$, Fe_2NiO_3Zn, $BaFe_{12}O_{19}$, and $SrFe_{12}O_{19}$), in which the average diameter of nano particles is less than 40nm were purchased from Sigma-Aldrich, Inc for measurement purposes employing this technique. For industrial benefits, we present the complex permeability and permittivity on the frequency range from 3.95GHz to 5.85GHz. The measured results showed that the dielectric permittivity of these materials is quite different from those of solid state materials.**

***Index Terms* — Nano ferrites, waveguide technique, permeability, permittivity.**

I. INTRODUCTION

The transmission and reflection technique was used in the free space measurement technique [1, 2]. The S-matrix analysis was also deployed for the coaxial [3] and rectangular [4, 5] waveguide techniques. These measurements are very reliable when it comes to measure the complex permeability and permittivity. However, the minimum diameter requirement of Gaussian beams in free space measurement always requires a wavelength for operating at a central frequency. In order to avoid diffraction errors from target materials, the surface diameter of the target material was at least three times larger than the diameter of the Gaussian beam. This implies that in order to determine a material's electro-magnetic properties at lower frequencies, a large amount of material is needed in the measurement process. Due to the relatively expensive and nominal nature of nano materials, a cost effective measurement technique requires the use of as little of the sample as possible. The waveguide technique fits the requirements for this and delivers very accurate results. It is obvious that each waveguide has a limited frequency band; however, they do not suffer radiation loss like free space measurements except for the attenuation losses of specific modes in the waveguide. In order to remove any unwanted losses from the waveguide, we applied a standard TRL calibration [4] technique to achieve a zero reference plane for the measurements inside the waveguide. After a great number of trials using TRL calibration, we noticed that one has to take into account the loaded material's permittivity and permeability effect into the cutoff wavelengths from the free space waveguide. In addition, the loaded material's thickness must be as thin as possible at lower frequency measurements in order to maintain the recommended insertion phase regime by Agilent. For this purpose, we present a modified reflection and transmission formulation for in-waveguide measurements. Also, a modified permeability and permittivity formulation from the modified propagation constant of the loaded waveguide is presented. Our studies show that this modification is necessary, and the derived permeability and permittivity data is very reliable and not affected by the scattering voltage ratios of the vector network analyzer.

II. THEORY AND MEASUREMENT

A propagating electromagnetic wave inside the waveguide is being reflected, S_{11}, and transmitted, S_{21}, by the loaded material. A diagram of this setup can be seen in Fig.1. The known electric and magnetic polarization of propagating waves in waveguides is very useful in analyzing the physical properties of certain materials. It is also very useful in determining the dielectric and magnetic complex permeability and permittivity of these materials.

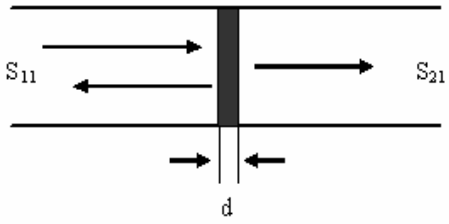

Fig.1 Schematic diagram of powder sample in waveguide

In this waveguide measurement technique, the standard TRL calibration applies to the zero reference plane findings. The zero reference planes were realized by the typical quarter

wavelength difference (l) between *thru* and *line* in air. The recommended insertion phase ranges from 20^0 to 160^0 are retained by proper TRL calibration. In order for the insertion phase contributions from air to be removed from the actual transmission line for the loaded material measurements, the thinly prepared target materials were loaded inside the waveguide and mounted onto the zero reference plane side. The modified S parameters are as follows:

$$\begin{aligned}\tilde{S}_{11} &= S_{11}e^{j(0\times\sqrt{k_0^2-k_c^2})} \\ \tilde{S}_{21} &= S_{21}e^{j(l-d)\times\sqrt{k_0^2-k_c^2}}\end{aligned} \quad (1)$$

Return losses of less than -50 dB from the air inside the waveguide are easily achieved using the calibration techniques described. This enables us to neglect any unwanted reflections from the inner walls of the waveguide when analyzing the S parameters. The reflection and transmission by the scattering parameters inside the waveguide, in which the transmission and reflection may be resembled by free space formulations, can now be presented as follows:

$$\begin{aligned}\Gamma &= K \pm \sqrt{K^2-1} \\ K &= \frac{\tilde{S}_{11}^2 - \tilde{S}_{21}^2 + 1}{2\tilde{S}_{11}} \\ T &= \frac{\tilde{S}_{11} + \tilde{S}_{21} - \Gamma}{1-(\tilde{S}_{11}+\tilde{S}_{21})\Gamma}\end{aligned} \quad (2)$$

The transmission coefficient through the material may also be written as follows: $T = e^{-\gamma d} = e^{-(\alpha + j\beta)d}$. The propagation constant through the material inside the waveguides can be derived to be:

$$\gamma_{TE_{10}} = \frac{\ln(\frac{1}{|T|})}{d} + j\left(\frac{2\pi n - \varphi_T}{d}\right) \quad (3)$$

Normally, a sample thickness of less than one quarter wavelength is desirable in this calibration, because it will make n = 0. In order to achieve our goal and derive the complex permeability and permittivity for the loaded material inside the waveguide, we must determine the propagation constant through the materials in the waveguide. To achieve this one must solve Maxwell's equations with respect to E_y for the TE_{10} mode as seen in Fig.2.

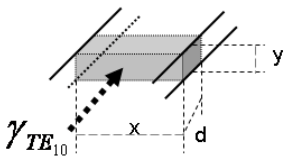

Fig.2 Propagating TE_{10} wave inside waveguide and the loaded material

$$(\frac{\partial}{\partial x'^2} + \frac{\partial}{\partial y'^2} + \beta^2)E_y = 0 \quad (4)$$

Where $x' = x\frac{1}{\sqrt{\mu\varepsilon}}$ and $y' = y\frac{1}{\sqrt{\mu\varepsilon}}$.

Solving Maxwell's equation leads to the following:

$$E_y = C\sin(\beta_x x')\cos(\beta_y y') \quad (5)$$

C is a constant to be determined from boundary conditions. The boundary condition tells us that the propagation constant components may be presented as follows: $\gamma_0 = \frac{2\pi}{\lambda_0}$, $\beta_x = \frac{n\pi}{a}\sqrt{\mu\varepsilon}$ and $\beta_y = \frac{m\pi}{b}\sqrt{\mu\varepsilon}$. This results in the following relationship for the total propagation constant through the material inside the waveguide: $\gamma^2 = \gamma_0^2 - \beta_x^2 - \beta_y^2$. The propagation constant of the TE_{10} can subsequently be written as follows:

$$\begin{aligned}\gamma_{TE_{10}} &= j2\pi\sqrt{\left(\frac{1}{\lambda_0}\right)^2 - \left(\frac{1}{2a}\right)^2}\cdot\sqrt{\mu\varepsilon} = j\gamma_{TE_{10}}^0\frac{\mu}{\eta} \\ \gamma_{TE_{10}}^0 &= \sqrt{\left(\frac{1}{\lambda_0}\right)^2 - \left(\frac{1}{2a}\right)^2}\end{aligned} \quad (6)$$

The complex permeability and permittivity associated with the propagation constant are:

$$\mu = \frac{\eta\gamma_{TE_{10}}}{j\gamma_{TE_{10}}^0} = -j\left(\frac{1+\Gamma}{1-\Gamma}\right)\left(\frac{1}{2\pi d}\right)\left(\frac{\ln(\frac{1}{|T|}) + j(2\pi n - \varphi_T)}{\sqrt{\left(\frac{1}{\lambda_0}\right)^2 - \left(\frac{1}{2a}\right)^2}}\right) \quad (7)$$

In our waveguide measurement technique the propagating wave inside the waveguide was assumed to be the TE_{10} mode. This implies that the propagating wave detects the permeability directly. However, the permittivity is detected indirectly and can be derived as follows:

$$\varepsilon = \frac{\mu}{Z_{TE}^2} = \frac{\mu}{\eta^2}\left(\lambda_0^2\left(\frac{1}{\lambda_0^2} - \frac{1}{4a^2}\right)\right) \quad (8)$$

$$\varepsilon = -j\left(\frac{c}{f}\right)^2\left(\frac{1-\Gamma}{1+\Gamma}\right)\left(\frac{1}{2\pi d}\right)\left(\ln(\frac{1}{|T|}) + j(2\pi n - \varphi_T)\right)\left(\sqrt{\left(\frac{1}{\lambda_0}\right)^2 - \left(\frac{1}{2a}\right)^2}\right) \quad (9)$$

The equations above are used to calculate the complex permeability and permittivity of samples inside the waveguide. Now we present the measured complex

permeability and permittivity of nano ferrite materials using this waveguide technique.

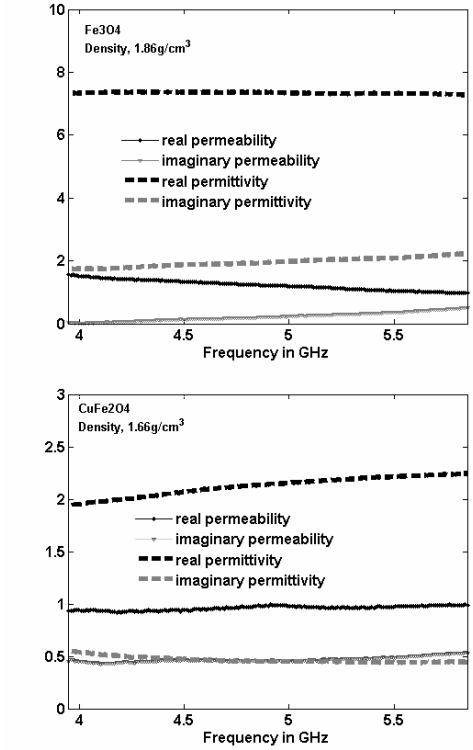

Fig.1 Complex permeability and permittivity measurements of pure spinel nano ferrites

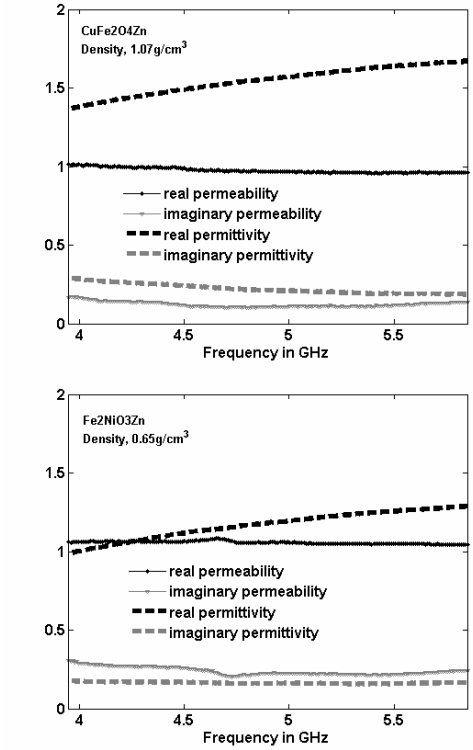

Fig.2 Complex permeability and permittivity of cation substituted spinel nano ferrites

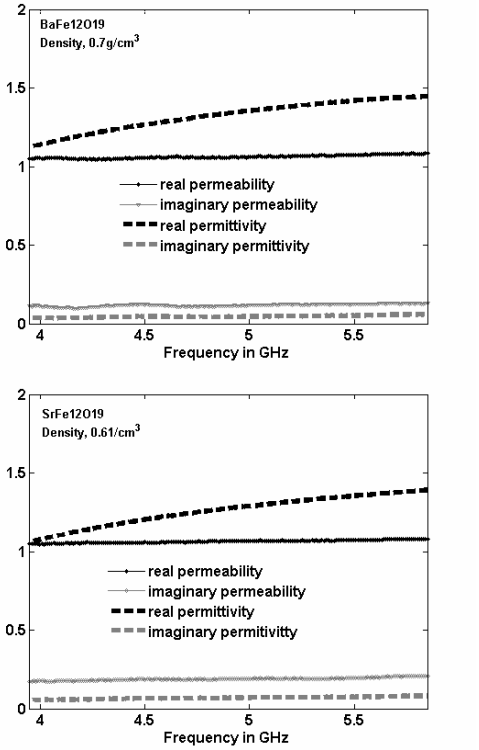

Fig.3 Complex permeability and permittivity measurements of nano hexaferrites

For the purposes of a brief comparison, we simply recalled the previous studies using waveguide measurements where cutoff wavelengths were not accounted for in the permeability and permittivity measurements and the technique proposed in this paper demonstrates our ability to successfully account for the effect of the cutoff frequencies and obtain the potential permeability and permittivity (see fig.4).

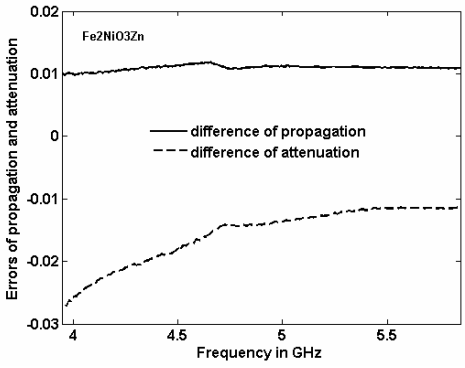

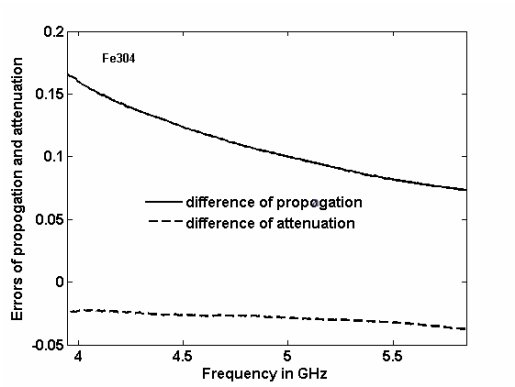

Fig.4 Free space cutoff wavelengths over contributions to the propagation and attenuation

Compared to previously published data, the data obtained using the new proposed technique is superior. As expected, the propagation difference between our technique and one that doesn't account for cut-off wavelengths is small for the low permeability and permittivity material of Fe_2NiO_3Zn. However, for Fe_3O_4, which has a considerably higher permittivity and permeability, the difference in propagation constants is very significant. This leads one to believe that the complex parameters from propagation constants of previous analysis might be overestimated. Through the analysis we have noticed that the recommended phase can be maintained for high permeability and permittivity materials by loading thinner samples. This implies that the measurement could be very successful for films such as carbon nanotube due to the fact that the partial insertion phase region is able to prove the reflection and transmission theories of S-matrices using a two port vector network analyzer.

III. Conclusion

1. In the measurements in Fig.1, the nano powders of Fe_3O_4 demonstrated a high real permittivity and a higher associated imaginary component. This may be due to the semi conductive behavior of this material. The nano powder, $CuFeO_4$, demonstrated relatively less complex permittivity compared to Fe_3O_4.
2. In Fig.2, the cations (Ni and Zn) substituted nano spinel ferrites demonstrated a smaller loss in their permittivity and permeability when compared to Fe_3O_4 and $CuFeO_4$. The real part of their permittivity is also smaller than that seen in Fig.1. This may be due to the diluted density of the materials as well as the intrinsic behavior of the material itself.
3. In Fig.3 the nano hexaferrites with high resistivity and anisotropic energy demonstrated low loss and low permittivity behavior. The real parts of their permittivity react very slightly to an increase in frequency. These nano hexaferrites have a permittivity that is close to air and can be accredited to excellent powder engineering.
4. In all the measurements of complex permeability of the nano ferrite powders, the permeability is very close to that of air. This may be due to the fact that the 40nm nano ferrites are already in a super paramagnetic state.
5. According to the Fig.6, the permeability and permittivity effect into cutoff wavelengths should be seriously considered for accurate measurements.

ACKNOWLEDGEMENT

The authors wish to acknowledge the support of US Army contract, security agent.

REFERENCES

[1] D. K. GHODGAONKAR, V. R. VARADAN, and V. K. VARADAN, IEEE transactions on instrumentation and measurement, Vol. 39, NO. 2, April 1990.
[2] Rene Grignon, Mohammed N. Afsar, Yong Wang and Saquib Butt, IMTC 2003-Instrumentation and Measurement Technology Conference, Vail CO, USA, 20-22 May 2003.
[3] Madhan Sundaram, Yoon Kang, S. M. Shajedul Hasan, and Mostofa K. Howlader, SNS-CONF-ENGR-133
[4] Y. Wang and M. N. Afsar, Progress In Electromagnetics Research, PIER 42, 131-142, and 2003.
[5] Achmad MUNIR, Noriaki HAMANAGA, Hiroshi KUBO, and Ikuo AWAI, IEICE Trans. Electron., Vol.E88-C, NO.1 JANUARY 2005.